PHYSICAL REVIEW E, VOLUME 65, 036138

Model for glass transition in a binary fluid from a mode coupling approach

Upendra Harbola and Shankar P. Das
School of Physical Sciences, Jawaharlal Nehru University, New Delhi 110067, India

(Received 28 August 2001; published 6 March 2002)

We consider the mode coupling theory (MCT) of glass transition for a binary fluid. The equations of nonlinear fluctuating hydrodynamics for the compressible fluid are obtained with a proper choice of slow variables which correspond to the conservation laws in the system. The resulting model equations are used to obtain a coupled set of nonlinear integro-differential equations for the various correlations of partial density fluctuations. These equations are then solved self consistently in the long-time limit to locate the dynamic transition in the system. The transition point from our model is at considerably higher density than predicted in the other existing MCT models for binary systems.

DOI: 10.1103/PhysRevE.65.036138 PACS number(s): 64.60.Cn, 64.70.Pf, 05.60.−k, 47.35.+i

I. INTRODUCTION

The phenomenon of glass transition has been studied widely in recent years using the mode coupling models obtained from a microscopic theory of the liquid state. This involves a nonlinear feed back to the transport properties of the liquid resulting from the coupling of hydrodynamic modes in the system. Thus the crucial result of mode coupling theory (MCT) [1] consists of a self consistent expression for the generalized transport coefficients in terms of the couplings of slowly decaying density fluctuations. With the simplest form of the coupling, the system undergoes a dynamic transition to a nonergodic state as the density increases beyond a critical value. Here the long-time limit of the time correlation of density fluctuations are treated as an order parameter for structural relaxation. In analogy with spin-glass models [2] this dynamic transition is characterized by a nonzero value of the order parameter or the so-called Nonergodicity parameter (NEP). Besides approaching the problem from basic theoretical models [3] using statistical mechanics, computer simulation has proved to be a very useful tool for the study of glassy behavior. The equations of motions for a system of particles moving under classical laws of motion with simple interaction potentials like hard spheres or the Lennard-Jones type has been studied [4,5]. In such simulations the binary mixtures of different types of particles are usually considered since two-component systems seem to avoid the crystallization and continue to remain in the disordered state until very high density.

For a binary system the self-consistent MCT for glass transition and the dynamic instability resulting from the feedback mechanism have been studied by several authors [6,7] in the past. Analysis of the data were made through schematic models or by treating the various nonuniversal parameters in the theory as freely adjustable for fitting. However the existing model with wave-vector dependence predict the dynamic transition at a much lower density compared to the one where a structural arrest is seen in computer simulation of similar systems. This aspect of the mode coupling model for the binary fluid was indicated in the computer simulation results reported in Ref. [8]. These authors simulated a binary Lennard-Jones system and the tendency to freeze occurred at much lower temperature than what one would expect from the existing versions of the MCT on binary systems. In the present paper, we go back to the basic formulation of the theory. We use the nonlinear fluctuating hydrodynamics (NFH) approach to the problem for this. Results obtained for one-component systems in similar analysis has provided important insight into the problem in previous works [9,10]—where it was first shown that the consideration of the full set of equations for the compressible fluid finally restores ergodicity in the system. In the present calculation for two-component fluids we will focus mainly on the dynamic instability as a first step and analyze the implications of the feedback mechanism of MCT as the central issue.

The first step in the construction of the proper equations for the fluctuating nonlinear hydrodynamics involves identification of the correct set of slow variables for the system. The binary systems have a set of conservation laws which are different from the one-component fluids. The conservation laws for the two-component system involve the individual densities and the total momentum density of the particles. The individual momentum densities are not conserved quantities. This has important implications on the dynamical behavior that we will consider in the present paper. In constructing the NFH equations for the binary fluid the proper free-energy functional in terms of the slow variables is also needed. We compute this from the microscopic Hamiltonian of the binary mixture by considering the classical partition function for the system. This is done following the method of Langer and Turski [11]. The so-called interaction part of the free energy is taken in the standard form with expansion in terms of direct correlation functions [12]. Our equations at the linearized level are similar to those of fluctuating hydrodynamics in the literature [13,14]. The nonlinearities that give rise to the mode coupling transition come from the reversible part involving the pressure term in the momentum conservation equation. The Poisson bracket relations between the microscopic variables are used in obtaining the reversible part or the Euler terms in the fluctuating equations. Our equations agree at the linear level with earlier formulation of linearized hydrodynamics of binary systems by Cohen *et al.* [13]. We consider the correction to the transport coefficient coming from the nonlinearities within the standard form of mode coupling approximation of dominant density fluctuations. The self-consistent expression for the correlation functions constitute the feedback mechanism for the transport properties. The possible dynamic transition allowed by the model equations is analyzed in terms of the solution of the resulting integral equations. In the computation of the mode coupling integrals that appear in the renormalized form of the transport coefficients, the static structure factor of the liquid is required as an input. This appears through the direct correlation functions in the driving free-energy functional which in turn determines the nonlinearities in the equations of motion. In the present paper, we confine ourselves to a strictly Gaussian type free-energy functional. The necessary two-point direct correlation functions can be expressed in terms of static structure factors for the binary mixture through Ornstein-Zernike relations. The thermodynamic properties of the fluid determined from the interaction potential of the particles thus enters the formulation of the dynamics. In the one-component case the Percus-Yevick (PY) structure factor has been used mostly for this purpose. In the case of the binary mixtures we use the extension of the PY models for a two-component fluid by Lebowitz. These structure factors are obtained as a function of the size ratio (α) and the relative abundance of the species denoted by the variable x.

Our main findings are very different from the existing results [16]. From the self-consistent solution of these nonlinear integral equations, we find that dynamic transition occurs at much higher densities than predicted by other existing models [6,15,16] for the same system. The theoretical prediction for the critical density of the dynamic transition is now in better quantitative agreement with the computer simulation results. In order to clearly indicate the difference of the present paper from existing MCT for binary systems, we will discuss here—under what approximations the present paper reduces to those models. The present approach gives rise in a very natural way the interesting features of the glassy behavior in a two-component system where the dynamics of one species take place in the presence of another. This situation become particularly different from a one-component system, in strong asymmetry of the two species. The occurrence of freezing or jamming in the supercooled liquid is sensitive to the size ratio of the species as well as the relative abundance. Thus for example if one of the species is too small compared to its counter part, the smaller ones move in the matrix of the bigger particles and hence avoid the freezing to high density. Indeed we see such behavior from the analysis of the model presented here. However, when the proper limits of the compositions and sizes of the two species in the binary mixtures are considered, the transition point obtained from our model is equal to that of an one-component system [17], as is expected.

This paper is organized as follows. In the next section, we describe our model and obtain the nonlinear fluctuating hydrodynamic equations for the slow variables. We then present various correlation functions in the linearized dynamics. We also indicate the equivalence of the present formulation with earlier works of linear fluctuating hydrodynamics. In Sec. III, we discuss the effects of the nonlinearities and obtain the integral equations for the nonergodicity parameters signifying the feedback mechanism. In Sec. IV, we demonstrate how the present paper can obtain the other existing MCT models in the literature. The implications of this paper on the dynamic transition is analyzed in the next section with presentation of the results. We end the paper with a discussion of the results.

II. THE MODEL STUDIED

The slow variables for a binary fluid are the two-partial densities $\rho_s(\vec{x}), s=1,2$ and total momentum density $\vec{g}(\vec{x})$, respectively, representing conservation of the two species. The mass densities are defined microscopically as,

$$\rho_s(\vec{x}) = m_s \sum_{\alpha=1}^{N_s} \delta(\vec{x}-\vec{R}_s^{\alpha}(t)) \qquad (2.1)$$

where $\vec{R}_s^{\alpha}(t)$ is the position of the αth particle in the sth species. The momentum densities $\vec{g}_s$ for the two species can be represented similarly as,

$$\vec{g}_{is}(\vec{x}) = \sum_{\alpha=1}^{N_s} \vec{P}_{is}^{\alpha}\delta(\vec{x}-\vec{R}_s^{\alpha}(t)) \qquad s=1,2, \qquad (2.2)$$

where $\vec{P}^{s}_{\alpha}$ is the momentum of the αth particle in the species s (=1 or 2) and N_s is the number of particles in the sth species in the mixture. The total number of particles is given by $N=\Sigma_s N_s$. We ignore the energy fluctuations to keep the analysis simple. In a binary fluid the total momentum conservation gives rise to the slow variable $\vec{g}=\vec{g}_1+\vec{g}_2$. In writing the equations for the dynamics of the slow variables consisting of the set $\{\rho_1,\rho_2,\vec{g}\}$ we use the standard procedure [18,10] to obtain the generalized Langevin equations. The reversible or the Euler part is written in terms of the Poisson brackets [19] between the slow variables. Using the basic Poisson bracket (PB) relation, $\{R_s^{\alpha},\vec{P}_{s'}^{\beta}\}=\delta_{ss'}\delta_{\alpha\beta}$, we obtain the following PB's among the slow variables,

$$\begin{aligned}\{\rho_s(\vec{x})g_i(\vec{x}')\} &= -\nabla_i[\delta(\vec{x}-\vec{x}')\rho_s(\vec{x})],\\ \{g_i(\vec{x})g_j(\vec{x}')\} &= -\nabla_j[\delta(\vec{x}-\vec{x}')g_i(\vec{x})]\\ &\quad +\nabla'_i[\delta(\vec{x}-\vec{x}')g_j(\vec{x}')].\end{aligned} \qquad (2.3)$$

The free-energy functional, F, that is used in constructing the equations of the nonlinear fluctuating hydrodynamics plays an important role here. It has two parts, the kinetic and the "potential," respectively, denoted by F_k and F_u,

$$F=F_k+F_u. \qquad (2.4)$$

In obtaining the form of the free-energy functional in terms of the slow variables $\vec{g}$ and ρ, we follow the standard procedure due to Langer and Turski [11]. The details of this deduction beginning from a microscopic Hamiltonian for the binary fluid is presented in the Appendix. The kinetic part F_k, is obtained in terms of the hydrodynamic variables as

$$F_k=\frac{1}{2}\int d\vec{x}\,\frac{g^2(\vec{x})}{\rho(\vec{x})}, \tag{2.5}$$

where the total density $\rho=\rho_1+\rho_2$ appears in the denominator of Eq. (2.5). It should be noted that this expression is different from Eq. (4.5) in general. This is essential for generating the Galilean invariant form of the generalized Navier-Stokes equation obtained for the momentum density $\vec{g}$. For the potential part F_u of the free-energy there is an ideal-gas contribution together with the interaction term, $F_u=F_{id}+F_{int}$. The ideal-gas part F_{id} follows from the procedure sketched in the Appendix and for F_{int} we use the standard form [12,20] in terms of the direct correlation functions. Thus F_u is obtained as

$$F_u(\rho)=\frac{1}{m_s}\int d\vec{x}\,\rho_s(\vec{x})\left[\ln\frac{\rho_s(\vec{x})}{\rho_{os}}-1\right] -\frac{1}{2m_sm_{s'}}\int d\vec{x}\,d\vec{x}\,'\,c_{ss'}(\vec{x}-\vec{x}\,')\,\delta\rho_s(\vec{x})\,\delta\rho_{s'}(\vec{x}\,'), \tag{2.6}$$

where ρ_{os} is the average density of the sth species in the mixture and $c_{ss'}(\vec{x})$ represents the equilibrium two-particle direct correlation function [21] between s and s'.

Using standard methods, the generalized Langevin equations for the slow variables are obtained as

$$\frac{\partial\rho_s}{\partial t}+\nabla\cdot\left[\frac{\rho_s}{\rho}\vec{g}\right]+\gamma_{ss'}\frac{\delta F_u}{\delta\rho_{s'}}=\theta_s,\qquad s=1,2, \tag{2.7}$$

$$\frac{\partial g_i}{\partial t}+\nabla_j\frac{g_ig_j}{\rho}+\rho_s\nabla_i\frac{\delta F_u}{\delta\rho_s}+L_{ij}\frac{\delta F}{\delta g_j}=f_i, \tag{2.8}$$

where the repeated indices are summed over—a convention that we will follow in the rest of the paper. The bare transport coefficient L_{ij} for the momentum current density correspond to the viscosity tensor given by

$$L_{ij}(\vec{x})=-\eta_o\left(\frac{1}{3}\nabla_i\nabla_j+\delta_{ij}\nabla^2\right)-\zeta_o\nabla_i\nabla_j, \tag{2.9}$$

where η_o and ζ_o are bare shear and bulk viscosities, respectively. The longitudinal viscosity is given by $\Gamma_o=(4\eta_o/3+\zeta_o)/\rho_o$. The $\gamma_{s's}$ correspond to the inter- and self-diffusion in the two species. We use the expression [20] $\gamma_{s's}\equiv\partial_i\gamma_{s's}^{ij}\partial_j$. On adding the equations (2.7) with $s=1,2$ for the two-components, the continuity equation $\partial\rho/\partial t+\nabla\cdot\vec{g}=0$ for the total density $\rho(=\rho_1+\rho_2)$ is obtained. Thus the diffusion kernel in the first two equations of (2.7) for $s=1,2$ should cancel. We will use the simple choice here that $\gamma_{21}=-\gamma_{11}\equiv\gamma_o\nabla^2$ and $\gamma_{12}=-\gamma_{22}\equiv\gamma_o\nabla^2$. The noise in the respective equations is assumed to be white Gaussian and related to the corresponding bare transport coefficients as

$$\langle\theta_s(\vec{x},t)\,\theta_{s'}(\vec{x}\,',t')\rangle=2k_BT\gamma_{ss'}\,\delta(\vec{x}-\vec{x}\,')\,\delta(t-t'), \tag{2.10}$$

$$\langle f_i(\vec{x},t)f_j(\vec{x}\,',t')\rangle=2k_BTL_{ij}\,\delta(\vec{x}-\vec{x}\,')\,\delta(t-t'), \tag{2.11}$$

$$\langle\theta_s(\vec{x},t)f_i(\vec{x}\,',t')\rangle=0, \tag{2.12}$$

where s, s' denote type of species while i and j represent Cartesian axes. k_B is the Boltzmann's constant. Note that the noises corresponding to density fluctuations satisfies $\theta_1+\theta_2=0$ so that the total density satisfies the continuity equation. Thus there is only one independent noise. This is similar to earlier works [20,13] of fluctuating hydrodynamics on binary fluids. Thus, for example, instead of taking ρ_1 and ρ_2, one can construct the theory in terms of the variables $\rho=\rho_1+\rho_2$ and $c=x_2\rho_1-x_1\rho_2$, where $x_s=\rho_{os}/\rho_o$. The equation corresponding to ρ is just the continuity equation with $\vec{g}$ as the related current. The Langevin equation for c is a diffusive equation with a coupling to the total density ρ. This is similar to the works of linearized hydrodynamics existing in the literature [14]. The relation between the noises in the equations for the two different densities, i.e., ρ_1 and ρ_2 stated above is needed for the simple fact that the continuity equation is unchanged. A similar relation between noises was also used in earlier models of binary fluids [22,20]. With the present definition of the concentration c given above, the noise in the equation for c is the same as that for ρ_1 and ρ_2. The present choice of the set of slow variables, namely, ρ_1 and ρ_2 is made keeping in analogy with existing MCT models for binary systems [6]. Next we consider the linear equations of motion giving the correlation functions in terms of the bare transport coefficients. This is followed by the renormalization of the transport coefficient in the mode coupling approximation.

Linearized dynamics

The time correlation functions with linearized form of the dynamical equations given above are computed following standard procedure [23]. The MCT equations for the binary mixtures deal with the 2×2 matrix $C(q,t)$ of correlations of density fluctuations. The density correlation between the s and the s' species is defined as

$$C_{ss'}(\vec{x}-\vec{x}\,',t-t')=\frac{1}{N}\langle\delta\rho_s(\vec{x},t)\,\delta\rho_{s'}(\vec{x}\,',t')\rangle. \tag{2.13}$$

We denote the corresponding equal time quantity by the matrix χ. The Laplace transform of the density correlation functions is defined as

$$C_{ss'}(z)=-\iota\int dt\,e^{\iota zt}C_{ss'}(t)\qquad \mathrm{Im}(z)>0. \tag{2.14}$$

Following standard procedures [23] we obtain an equation for the correlation function matrix $C(q,z)$ as

$$[zI+M(q,z)]C(q,z)=\chi(q), \tag{2.15}$$

TABLE I. The matrix of $N_{ss'}(q,z)$ (see text) appearing in Eq. (2.18) for various density correlation functions.

$(z+M_{22})\chi_{11}-M_{12}\chi_{21}$	$(z+M_{22})\chi_{12}-M_{12}\chi_{22}$
$(z+M_{11})\chi_{21}-M_{21}\chi_{11}$	$(z+M_{11})\chi_{22}-M_{21}\chi_{12}$

where I is the identity matrix and the matrix M is given by

$$M(q,z)=q^2[\iota\overline{\gamma}+\{z+q^2\Gamma_o(q)\}^{-1}\tilde{\Delta}]\chi^{-1}(q). \quad (2.16)$$

$\Gamma_0(q)$ is the q-dependent bare longitudinal viscosity [20]. The matrices $\overline{\gamma}$ and $\tilde{\Delta}$ are given as

$$\overline{\gamma}_{ss'}=\gamma_0(-1)^{s+s'} \quad \text{and} \quad \tilde{\Delta}_{ss'}=\rho_o x_s x_{s'}. \quad (2.17)$$

Solving the set of equations (2.15) the correlation of different density fluctuations in the linearized form are obtained as

$$C_{ss'}(q,z)=\frac{N_{ss'}(q,z)}{D(q,z)}, \quad (2.18)$$

where functions $N_{ss'}(q,z)$ are given in Table I and $D(q,z)$ is given by,

$$D(q,z)=z^2+z\mathrm{Tr}\{M(q,z)\}+|M(q,z)|, \quad (2.19)$$

where $\mathrm{Tr}\{M(q,z)\}$ and $|M(q,z)|$ represent trace and determinant of the matrix $M(q,z)$, respectively. The equal time density correlation matrix $\chi(q)$ is expressed in terms of the commonly used quantity, the partial static structure factor $S_{ss'}(q)$ [21] of the system, as $\chi_{ss'}(q)=a_s a_{s'} S_{ss'}(q)$ where $a_s=m_s\sqrt{n_s}$, m_s and n_s are, respectively, mass and particle density corresponding to the sth species. An explicit expression for the partial structure factor $S_{ss'}(q)$, in terms of the direct correlation functions $c_{ss'}(q)$, is obtained from the solution of the generalized Percus-Yevick equation for a hard-sphere binary mixture [24,25].

III. FEEDBACK MECHANISM FROM DENSITY FLUCTUATIONS

In this section, we consider the implications on the dynamic transition as a result of the coupling of hydrodynamic variables. We compute the mode coupling contribution to the transport coefficients by treating the nonlinearities in equations of motion with standard methods [23]. The renormalized form for the longitudinal viscosity at the one-loop order is given by

$$\Gamma^{mc}(q,t)=\frac{1}{2\rho_0 q^2}\int\frac{d\vec{k}}{(2\pi)^3}V_{ss'}(q,k)V_{ll'}(q,k_1) \times C_{l's'}(k,t)C_{ls}(k_1,t), \quad (3.1)$$

where $k_1=q-k$. The vertex function $V_{ss'}(q,k)$ is given by

$$V_{ss'}(q,k)=(a_s a_{s'})^{-1}[(\hat{q}\cdot\vec{k})\tilde{c}_{ss'}(k)+\hat{q}\cdot\vec{k}_1\tilde{c}_{ss'}(k_1)]. \quad (3.2)$$

The quantity $\tilde{c}_{ss'}(q)=(n_s n_{s'})^{1/2}c_{ss'}(q)$ is related to the structure factor $S_{ss'}(q)$ through the Ornstein-Zernike relation $[\delta_{ls}-\tilde{c}_{ls}(q)]S_{ls'}(q)=\delta_{ss'}$. In obtaining the above expression (3.1) we have considered only the coupling of the density fluctuations coming from the nonlinearity in the pressure term that appears in the momentum conservation Eq. (2.8). This involves taking the density fluctuations as dominant and using the one-loop correction or the so-called Kawasaki approximation to the four-point functions to the transport coefficients. This is done in the same spirit of the self-consistent mode coupling approximation as taking density fluctuations to be dominant as in the case of one-component fluid. We would like to point out here that in the appropriate limit these results reduce to the one-component fluid result that *is in complete agreement* with all other wave-vector-dependent models [17] for one-component systems. The correlations of density fluctuations are now expressed in terms of the renormalized viscosity, $\Gamma^R(q,z)=\Gamma_0(q)+\int\Gamma^{mc}(q,t)e^{\iota zt}dt$. The ideal glass phase is characterized by the nonergodicity parameter, defined as

$$f_{ss'}(q)=\lim_{t\to\infty}\frac{C_{ss'}(q,t)}{\sqrt{\chi_{ss}\chi_{s's'}}}. \quad (3.3)$$

In the asymptotic limit of long-times, the correlation functions with renormalized transport coefficients reduces to a set of self-consistent equations for the NEP's $f_{ss'}(q)$,

$$f_{ss'}(q)=\frac{\mathcal{I}_{ss'}(q)\Gamma(q)}{1+\Omega(q)\Gamma(q)}. \quad (3.4)$$

Here $\Gamma(q)$ is the long-time limit of $\Gamma^{mc}(q,t)$ given by Eq. (3.1). $\Omega(q)$ and $\mathcal{I}(q)$ are given by

$$\Omega(q)=\Delta_{ss'}S_{ss'}(q) \qquad \mathcal{I}_{ss'}(q)=\frac{\Delta_{ij}S_{is}(q)S_{js'}(q)}{[S_{ss}(q)S_{s's'}(q)]^{1/2}} \quad (3.5)$$

with $\Delta_{ss'}=a_s a_{s'}/\rho_o$. Equation (3.4) constitutes a set of coupled nonlinear integral equations for the nonergodicity parameters $f_{ss'}$. The dynamic instability of the ideal glass transition in the binary system is then located from the *self-consistent* solution of Eq. (3.4) by an iterative method in a similar manner as in the one-component systems. The static structure factor goes as an input in the calculation. The interaction potential for the system enters the present theoretical description for the dynamics through this thermodynamic quantity.

An essential property of the glassy state is a finite shear modulus. When a low-density fluid is sheared, strain produced in it relaxes very quickly while an elastic solid can sustain the applied shear. The solidlike nature is manifested through the propagating shear modes. The behavior of the shear modes are studied through the transverse current-current correlation functions [26]. As a result of the mode coupling instability discussed here, time scales associated with the structural relaxations diverge. Due to this dynamic transition, in the ideal glassy phase, transverse current correlation function [20] develops propagating shear modes or transverse modes [27] over all length scales. The expression for the speed of shear waves (c_T) in the binary fluid can be obtained in terms of nonergodicity parameters in the following form:

$$c_T^2 = \frac{1}{60\pi^2}\sqrt{\frac{x_1 x_2}{n_1 n_2}} \int dk\, k^4 \tilde{c}'_{ll'}(k)\tilde{c}'_{ss'}(k) f_{s'l'}(k) f_{sl}(k) \times \sqrt{S_{ss}(k) S_{ll}(k) S_{s's'}(k) S_{l'l'}(k)}, \tag{3.6}$$

where $\tilde{c}'_{ss'}(q)$ denotes derivative of $\tilde{c}_{ss'}(q)$ with respect to wavevector q. Once the location of the ideal glass instability is found the speed of the transverse shear waves in the ideal phase is computed using Eq. (3.6).

IV. EXISTING MCT MODELS FROM THE PRESENT APPROACH

It has been argued that the existing MCT models [6,15,16] previously used by various other authors to study the supercooled dynamics and glass transition in binary mixtures, are obtained from a microscopic paper. In this section, we show that *with certain simplifications* the results of those MCT models can also be obtained within the context of fluctuating nonlinear hydrodynamics. For this we take the momentum densities of the individual species also as slow variables together with their mass densities. Thus we have four slow variables, $\rho_1, \rho_2, \vec{g}_1$, and $\vec{g}_2$. The microscopic definitions for the two mass and momentum densities are the same as those given in Eqs. (2.1) and (2.2). The Poisson bracket relations among the four conserved variables are now given as

$$\{\rho_s(\vec{x}) g_{is'}(\vec{x}')\} = -\nabla_i[\delta(\vec{x}-\vec{x}')\rho_s(\vec{x})]\delta_{ss'}, \tag{4.1}$$

$$\{g_{is}(\vec{x}) g_{js'}(\vec{x}')\} = \nabla'_i[\delta(\vec{x}-\vec{x}') g_{js}(\vec{x}')]\delta_{ss'} - \nabla_j[\delta(\vec{x}-\vec{x}') g_{is'}(\vec{x})]\delta_{ss'}.$$

The generalized Langevin equation corresponding to the four conserved variables are obtained as

$$\frac{\partial \rho_s}{\partial t} + \nabla \cdot \vec{g}_s = 0, \tag{4.2}$$

$$\frac{\partial g_{is}}{\partial t} + \nabla_j \frac{g_{is} g_{js}}{\rho_s} + \rho_s \nabla_i \frac{\delta F_u}{\delta \rho_s} + L_{ij}^{ss'} \frac{\delta F}{\delta g_{js'}} = \tilde{f}_{is}, \tag{4.3}$$

where $s=1$, 2. In writing Eq. (4.2), we have ignored the self-diffusion and interdiffusion of the two species. The density equations now only have the reversible parts calculated from the Poisson bracket relations (4.1), i.e.,

$$\vec{g}_s = \frac{\rho_s}{\rho}\vec{g}. \tag{4.4}$$

We take the *same* free-energy functional F given in Eqs. (2.4) as was used in our calculation. The potential part F_u is still given by Eq. (2.6), while the kinetic part F_k in Eq. (2.5) reduces to the form [20]

$$F_k = \int d\vec{x}\left[\frac{g_1^2}{2\rho_1} + \frac{g_2^2}{2\rho_2}\right]. \tag{4.5}$$

$L_{ij}^{ss'}$ are the bare transport coefficients which now form a 2×2 matrix for $s,s'=1,2$. The thermal noise $\vec{\tilde{f}}_s$ in the equations for the momentum density $\vec{g}_s$ follow the fluctuation dissipation relation to the bare transport coefficients

$$\langle \tilde{f}_{is}(\vec{x},t)\tilde{f}_{js'}(\vec{x}',t')\rangle = 2\, k_B T\, L_{ij}^{ss'}\, \delta(\vec{x}-\vec{x}')\,\delta(t-t'). \tag{4.6}$$

Renormalization to the bare transport coefficients, as a result of the nonlinearities in the equations for the momentum currents is computed within the self-consistent mode coupling approximations of dominant density fluctuations. To the one-loop order the contribution to the transport coefficient matrix is given by

$$\tilde{N}_{ss'}(q,t) = \frac{n}{2 n_s n_{s'}} \int \frac{d^3k}{(2\pi)^3} V_{s\mu\sigma}(q,k) V_{s'\mu'\sigma'}(q,k) \times C_{\mu\mu'}(k,t) C_{\sigma\sigma'}(k_1,t), \tag{4.7}$$

where $k_1 = q-k$ and $n(=n_1+n_2)$ is the total number density. The vertex $V_{s\mu\sigma}(q,k)$ is obtained as

$$V_{s\mu\sigma}(q,k) = \frac{n}{m_\mu m_\sigma}[\hat{q}\cdot\vec{k}\,\delta_{s\sigma} c_{s\mu}(k) + \hat{q}\cdot\vec{k}_1\,\delta_{s\mu} c_{s\sigma}(k_1)]. \tag{4.8}$$

Using the same procedure for computing the renormalized transport coefficients, a set of nonlinear integral equations for the long-time limit of the density correlation functions or the nonergodicity parameters are obtained. Denoting the long-time limit of the matrices $C_{ss'}(q,t)$ and $\tilde{N}_{ss'}(q,t)$, respectively, by the corresponding matrix $F(q)$ and $\tilde{N}(q)$, we obtain the matrix equation

$$F(q) = (1/q^2)\tilde{S}(q)\tilde{N}(q)[\tilde{S}(q) - F(q)], \tag{4.9}$$

where keeping an analogy with the notations used in the earlier works we have used, $\tilde{S}_{ij} = \sqrt{x_i x_j} S_{ij}$. The above equations are identical to the model equations used in earlier studies [7] and are also the same as those given in Refs. [6,15,16]. These results can thus be obtained also in the present paper as is demonstrated here. The transition point calculated by the above model lies quite below (lower densities) the values predicted by the molecular-dymamics simulations. We come back to the approximations done here in the Discussion section of this paper.

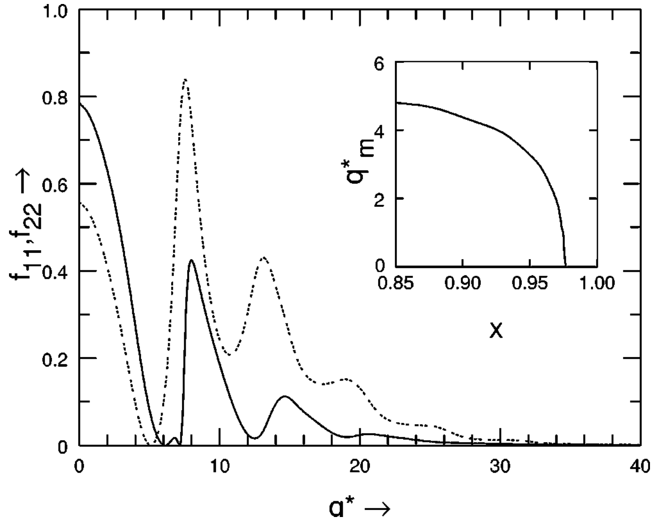

FIG. 1. Nonergodicity parameters $f_{11}(q^*)$ (solid line) and $f_{22}(q^*)$ (broken line) at $\eta_c=0.59$, $x=0.8$ and $\alpha=0.7$. $q^*=q\sigma_2$ is plotted along the x axis. Inset shows q_m^* (see text) vs x plot for $\alpha=0.8$ and $\eta=0.59$.

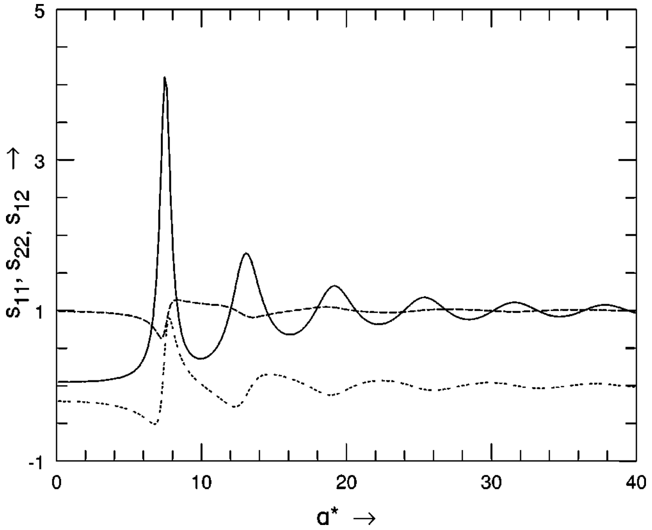

FIG. 2. Structure factors $S_{11}(q^*)$ (dashed), $S_{22}(q^*)$ (continuous), and $S_{12}(q^*)$ (dotted) are shown for the same thermodynamic parameters as given in Fig. 1.

V. RESULTS FOR THE DYNAMIC TRANSITION

Due to the available simple formulation for the structure and in order to keep continuity with pervious works on binary fluids [16] we will choose a mixture of hard spheres with equal masses. With this the binary system is described by three independent parameters, (a) the fractional concentration of bigger particles x, (b) the size ratio $\alpha(=\sigma_1/\sigma_2)$, of the diameters of the two species, and (c) the total packing fraction $\eta=\eta_1+\eta_2$ where η_1 and η_2 are the packing fractions of the individual species, $\eta_s=\pi/6n_s\sigma_s^3$. We take σ_2, the diameter of bigger species, as the unit of length. The structure factors for the binary liquid required in computing the mode coupling vertex functions appearing in Eq. (3.4) are obtained using the standard results of the solution of Percus-Yevick equations for the hard-sphere [25,24] mixture:

$$g_{ss'}(x)\left(e^{-\phi_{ss'}(x)/k_BT}-1\right)=e^{-\phi_{ss'}(x)/k_BT}\;c_{ss'}(x), \tag{5.1}$$

where $g_{ss'}(x)$ and $c_{ss'}$ are, respectively, the radial distribution functions and the direct correlation functions defined for a binary mixture. $\phi_{ss'(x)}$ is the pair potential among the particles of species of s and s'. This is computed for the special case of hard-sphere interaction [25] amongst the particles comprising the binary system such that

$$e^{-\phi_{ss'}(x)/k_BT}=0,\quad x<(\sigma_s+\sigma_{s'})/2=1\quad x>(\sigma_s+\sigma_{s'})/2. \tag{5.2}$$

We solve for the nonlinear integral Eqs. (3.4) to search the nontrivial fixed points with non zero values of NEP's $f_{ss'}(q)$. Depending on the thermodynamic parameters x,α, and η, described above, a nonergodic phase is seen beyond a critical density (η_c). The results remain unchanged if we replace x and α, respectively, by $1-x$ and $1/\alpha$ meaning an interchange of the label for the two species. In Fig. 1, we show the non-zero solutions for the NEP's f_{11} and f_{22}, respectively, for the critical packing fraction $\eta_c=0.59$. The nature of the ideal glass instability in the binary mixture is dependent on the size ratio α as well as the relative abundance x. We list below a few comments.

(i) The NEP f_{22} reaches a small value at an intermediate wave-number q_m depending on x (fraction of the bigger particles two). As the relative proportion x is increased this wave-number q_m becomes 0, beyond a value $x\geqslant x_0$. This behavior is primarily due to the nature of the structure function $\mathcal{I}_{ss'}(q)$ that appears in the mode-coupling equation (3.4) for the NEP's. In the inset of Fig. 1, we show how the position of $q_m^*=q_m\sigma_2$ shifts with x at $\alpha=0.7$ and becomes zero at $x_0=0.977$. Figure 2 shows the corresponding partial structures for different species.

In Figs. 3–5, we plot different nonergodicity parameters for a range of values of one of the three relevant thermodynamic parameters (x,α, and η) while keeping the other two fixed. With fixed x and α values, the amplitude of the various NEP's increases as we go deeper in to the glass phase with increasing η. This is shown in Figs. 3(a)–3(c). In Figs. 4(a)–4(c), we show the NEP's for a range of x values. We find that with increasing values of x, amplitudes of f_{11} and f_{12} decrease while that of f_{22} increases monotonically. In Figs. 5(a)–5(c), we have shown the NEP's, f_{11}, f_{22}, and f_{12}, for a range of α values at fixed $x=0.85$ and $\eta=0.60$. If the concentration (x) and the size of the bigger species is much larger than the smaller one we find that the NEP corresponding to the smaller species shows diffusive behavior. This is shown in Fig. 6 for $x=0.99$ and $\alpha=0.01$. This corresponds to the diffusion of the smaller particles through the matrix of the bigger species.

(ii) The transition to the nonergodic phase, indicating a structural arrest, shifts to higher densities as the size ratio (α) is decreased. For example, for $x=0.1$ and $\alpha=0.2$ *structural arrests are absent* up to very high densities ($\eta\leqslant 0.64$). This absence of transition here can be explained from the

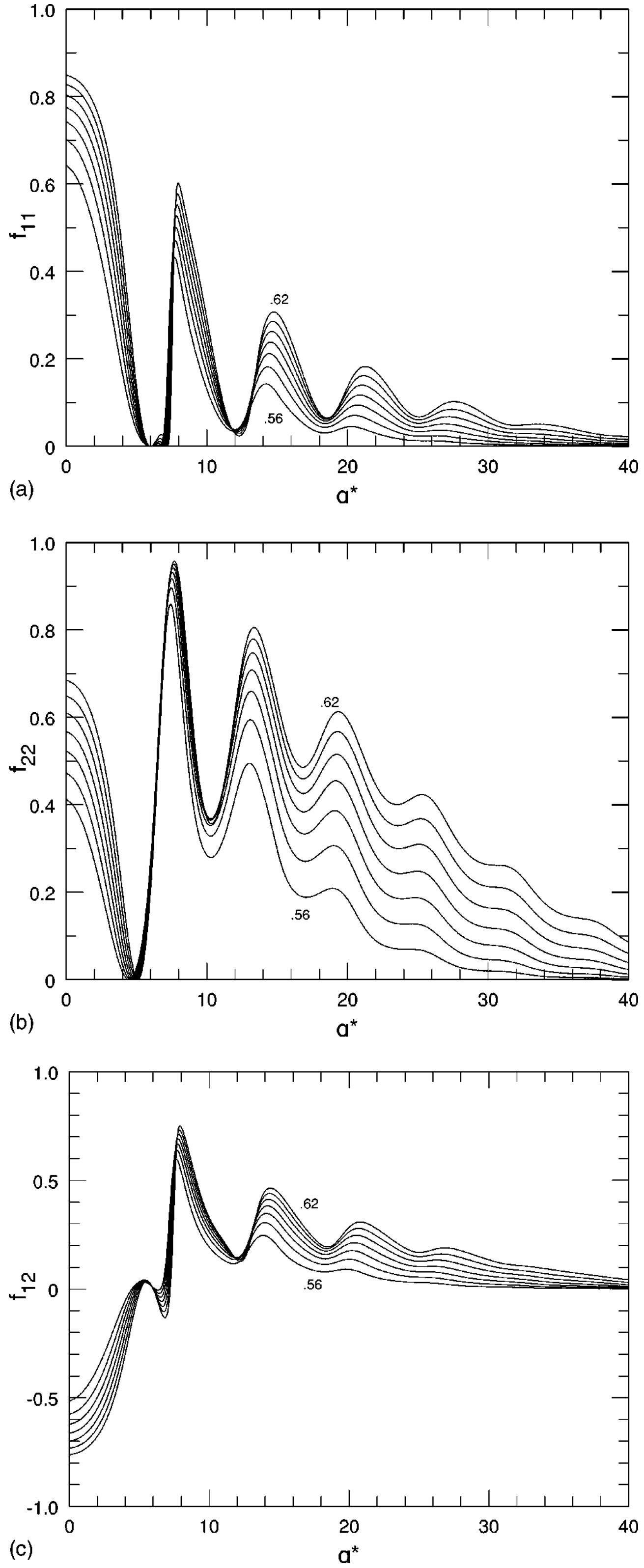

FIG. 3. Nonergodic parameters (a) $f_{11}(q^*)$, (b) $f_{22}(q^*)$, and (c) $f_{12}(q^*)$ for total packing fraction $\eta = 0.56$, 0.57, 0.58, 0.59, 0.60, 0.61, and 0.62 at fix $\alpha = 0.8$ and $x = 0.8$.

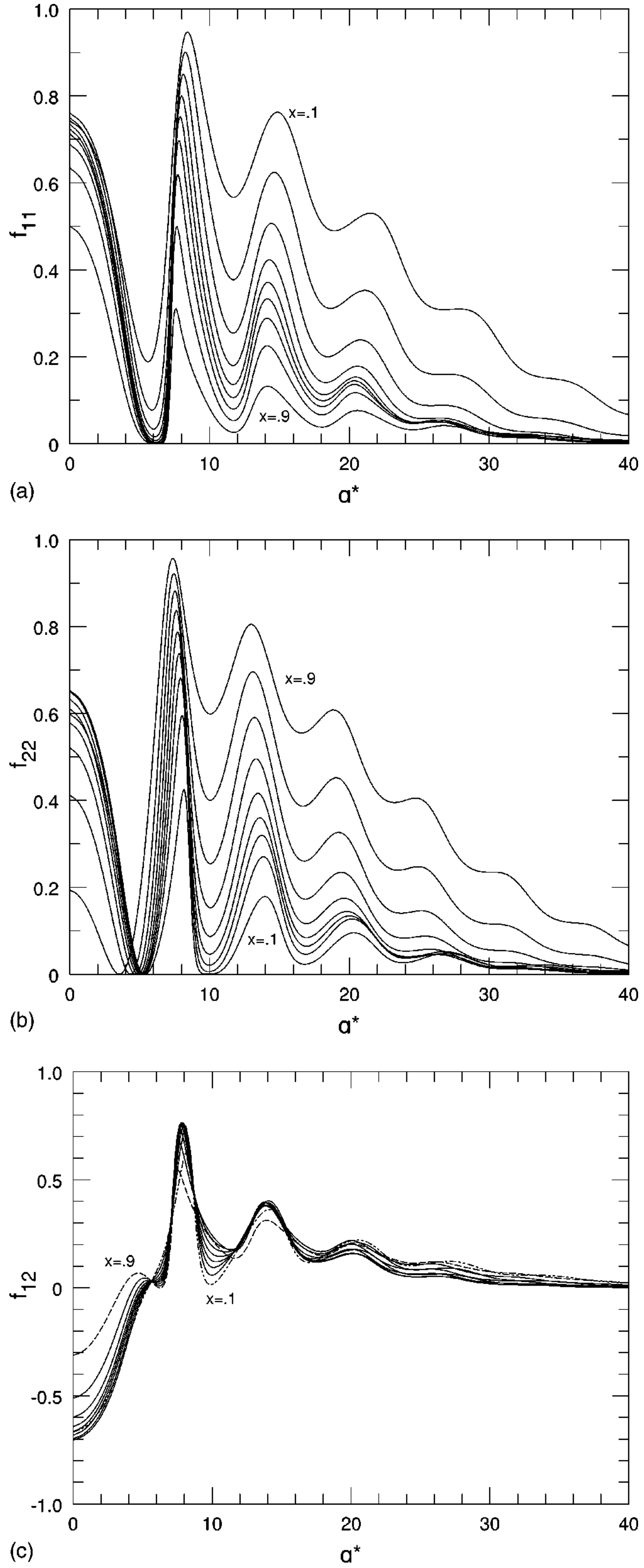

FIG. 4. Nonergodic parameters (a) $f_{11}(q^*)$, (b) $f_{22}(q^*)$, and (c) $f_{12}(q^*)$ at $\alpha = 0.85$ and $\eta = 0.57$. Different curves are for range $x = 0.1$, 0.2, 0.3, 0.4, 0.5, 0.6, 0.7, 0.8, and 0.9. In Fig. 4(c) only, curves corresponding to $x = 0.1$ and $x = 0.9$ are shown by dotted and dashed lines, respectively.

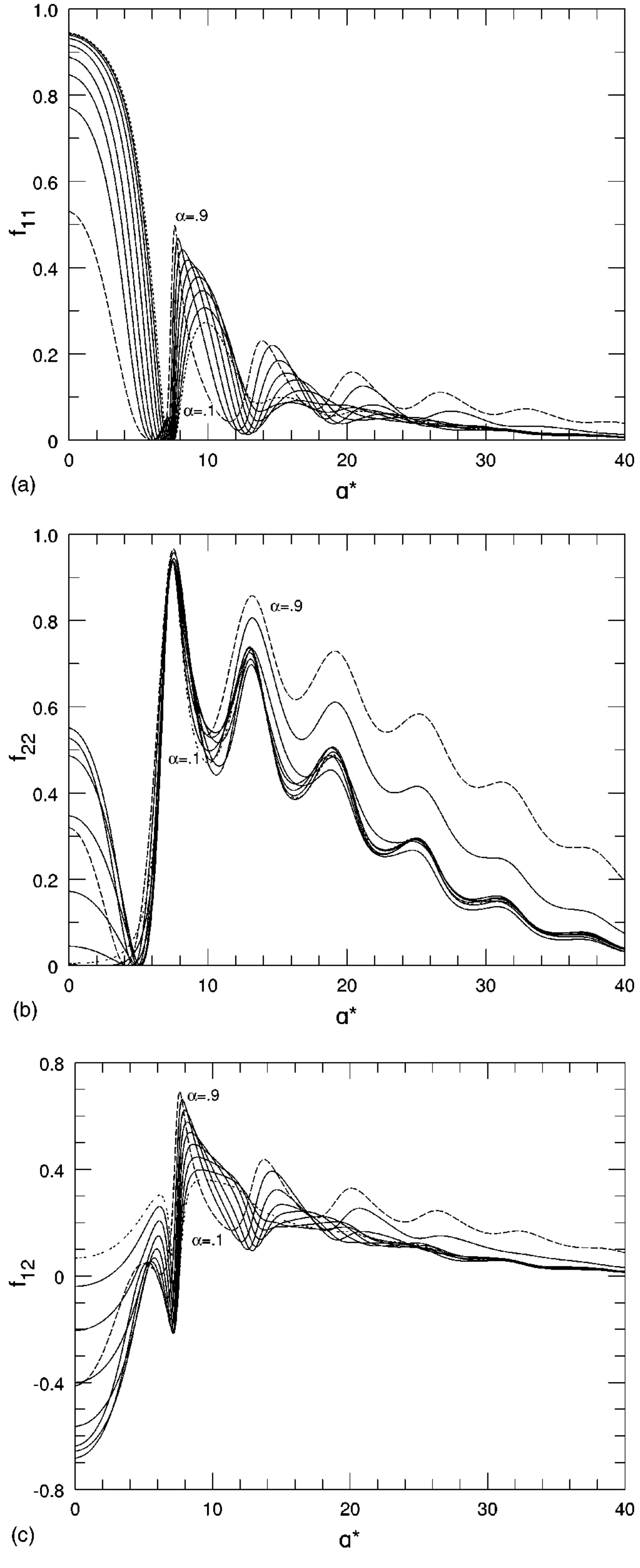

FIG. 5. Nonergodic parameters (a) $f_{11}(q^*)$, (b) $f_{22}(q^*)$, and (c) $f_{12}(q^*)$ at $x=0.85$ and $\eta=0.6$. Different curves are for range $\alpha=0.1$ (dotted), 0.2, 0.3, 0.4, 0.5, 0.6, 0.7, 0.8, and 0.9 (dashed).

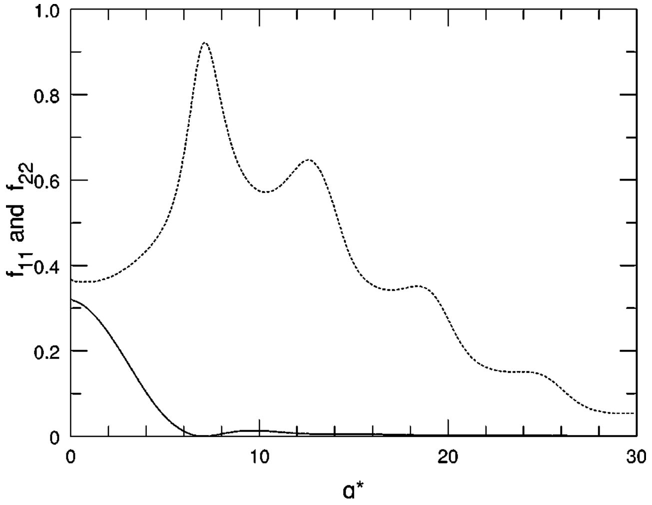

FIG. 6. Nonergodicity parameters $f_{11}(q^*)$ (continuous) and $f_{22}(q^*)$ (dotted) are shown for very small size ratio $(\alpha)=0.01$ and $x=0.99$ at $\eta_c=0.527$. The NEP f_{11} (corresponding to smaller particles) shows a diffusive character.

fact that for low values of x and size ratio α, the smaller particles can diffuse easily through the cage of the bigger particles and hence the structural arrest is avoided. Indeed it is a competition between the two quantities, the size ratio α allowing easier movement of the particles and x giving the relative abundance of the voids formed between bigger particles. To stress the importance of the present paper, it should be noted that, with the same values of the thermodynamic parameters Ref. [16] reports a transition in the range $(0.51 \leqslant \eta_c \leqslant 0.52)$. Figure 7 shows the variation of the critical packing fraction (η_c) with x at constant size ratio, $\alpha=0.8$.

(iii) With the ratio of particle sizes, α, smaller than 0.75, there is no structural arrest, over a range $(0.22 \leqslant x \leqslant 0.58)$. In the earlier mode coupling model equations [16] this sensitivity to the sizes of the particles (α) and (x) was absent. The same qualitative dependence of α on the freezing in a binary

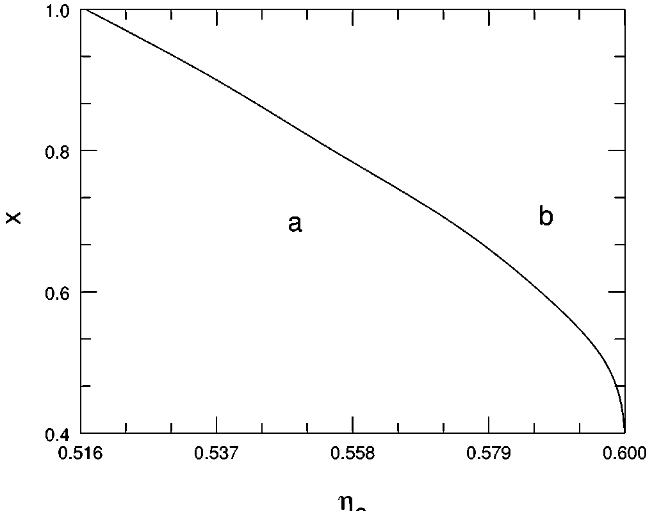

FIG. 7. Critical value of η_c is plotted with x for $\alpha=$ 0.8. Regions "a" and "b" represent liquid and glass phases, respectively.

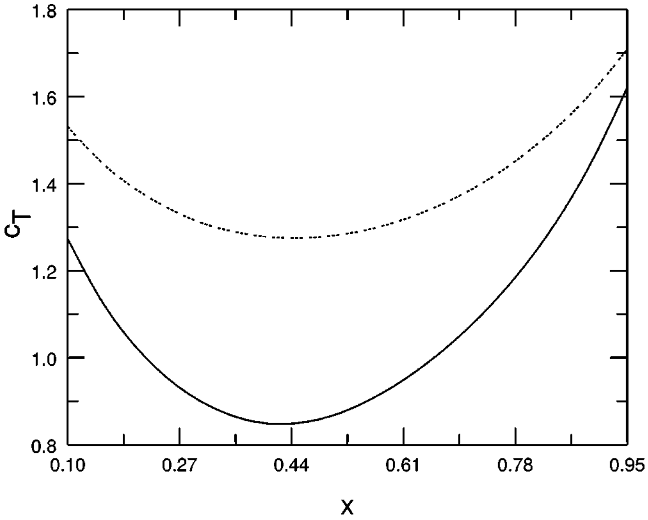

FIG. 8. Speed of shear mode c_T is plotted as a function of x for two values of $\alpha=0.85$ (solid) and 0.90 (broken) at $\eta=0.57$.

fluid system has also been reported in studies related to the thermodynamics [28] of the system.

If the particles are similar to each other ($\alpha=1$) and x close to unity, the dynamic instability occurs at $\eta=0.515$ that is very close to the critical packing fraction (with the use of the Percus-Yevick structure factor for binary systems) for a single-component system as is expected to be the case. In Fig. 8 we plot the speed of transverse mode (c_T) given by Eq. (3.6) as a function of x for two different size ratios (α) at constant total packing fraction, $\eta=0.57$.

VI. DISCUSSION

In the present paper, we have obtained, from the equations of nonlinear fluctuating hydrodynamics, the feedback mechanism of the self-consistent MCT. Solutions of our model equations indicate that the dynamic instability *shifts to much higher densities* than what is predicted in the earlier works [16]. This also agrees with the trend seen in computer simulation results [8]. The kinetic-energy term, Eq. (2.5), of the free-energy functional that is used here is crucial for the construction of the model equations. This is also essential for obtaining in the momentum conservation equation the convective or the so-called Navier-Stokes term reflecting Galilean invariance. In considering the dynamic nonlinearities that give rise to the mode coupling instability we have taken here a driving free-energy functional of Gaussian form. Thus, the origin of the nonlinearity is dynamic as is the case for the one-component fluid. The higher order terms in the free-energy functional will give rise to nonlinearities in the density equations and this will be required for the renormalization of the diffusion coefficients (γ_o). The lowest-order vertex then is proportional to the γ_o and will come from non-Gaussian terms in the free-energy functional involving higher-order direct correlation functions.

The main improvement resulting from the present formulation of the MCT for binary fluids comes from the consideration of diffusion between the two species. To demonstrate this we first note that from the standard fluctuation-dissipation relation (2.10), the average noise in the ρ_s equations contain a q^2 factor in the corresponding dissipation kernel. Thus the noise θ_s can be written down as $\theta_s = -\vec{\nabla}\cdot\vec{\alpha}_s$. With this substitution partial density equations can also be written as

$$\frac{\partial\rho_s}{\partial t}+\nabla\hat{\vec{g}}_s=0, \tag{6.1}$$

where $\hat{\vec{g}}_s$ can be understood as the current associated with the density of sth species and is given by,

$$\hat{\vec{g}}_s=\left[\frac{\rho_s}{\rho}\vec{g}\right]+\overline{\gamma}_{ss'}\vec{\nabla}\frac{\delta F_u}{\delta\rho_{s'}}+\vec{\alpha}_s. \tag{6.2}$$

Thus one can simply express Eq. (2.7) also in the for of a conservation equation. What is crucial to note here is that $\hat{\vec{g}}_s$'s individually are not conserved quantities but their sum is. The model used in our paper takes only the conserved quantities as slow variables. The dissipative and ther and omparts of the current $\hat{\vec{g}}_s$ in the two density equations, maintain a detailed balance to ensure the continuity equation. If the dissipative and the noise terms in Eq. (6.2) are ignored, the density equations have only contributions from the reversible parts and reduce to the form given by Eq. (4.4) in Sec. IV where we obtain the earlier MCT [6] models from the present paper. Note that in this case, the crucial kinetic-energy term in the free-energy functional reduces in terms of the slow variables $\vec{g}_1$ and $\vec{g}_2$ given by Eq. (4.5). We would like to stress here that no "microscopic" paper is necessary to get those equations used in earlier models. The crucial element that is missing is the interdiffusion. The model considered here brings in the interdiffusion in the dynamics and this is crucial in considering the phenomena of jamming or glass transition inthe binary systems. The resulting model equations show the relation between the size ratios and relative abundance of the two species and bring the theory closer to what is seen in simulations.

We end the paper with the following few comments.

(i) The earlier versions of the MCT [16] for binary systems can be reproduced from our paper, using the *same Gaussian free-energy functional*, if (a) the momentum densities of the individual components in the binary system, both treated as two *separately* slow variables with fluctuating equations and (b) ignore the interdiffusion denoted by γ among the species. This will also violate the Galileanin variance in the hydrodynamic equations.

(ii) Here we have considered the dynamics of density correlation functions only in the asymptotic limit so as to study the implications on the dynamic transition. The utility of the present paper is demonstrated through the better result for the location of the dynamic transition. To study the dynamics over different time scales the time-dependent mode coupling equations for the various density correlation functions have to be considered. These equations involve the bare transport coefficients γ_{ij} and L and will be reported elsewhere [29].

(iii) Finally, the complete picture of the dynamics will involve computing the coupling to the current correlations

[10] that restore the ergodicity in the longest time scale [29]. The present paper treats the long-time dynamics for the two-component system with the correct set of slow variables and shows quantitative agreement of MCT results with computer simulation studies and remedies the theories presented in earlier works.

ACKNOWLEDGMENTS

S.P.D. acknowledges support from NSF through Grant No. INT9615212. U.H. acknowledges financial support from the University Grant Commission, India.

APPENDIX

Here we present the calculation of the kinetic part, F_k, of the coarse-grained free-energy for a binary system starting from a microscopic Hamiltonian. The macroscopic system is divided in to cells of volume δ which is much larger than the average volume per particle while the linear dimensions of this volume (δ) are much smaller than the correlation length. The cell functions $\psi_a(\vec{R})$ are defined to be equal to unity if $\vec{R}$ is inside the ath cell or zero otherwise. The coarse grained partial densities and the total momentum inside the ath cell are

$$\rho_{sa}=\sum_{\alpha=1}^{N_s} m_s\psi_a(\vec{R}_s^\alpha) \quad \vec{g}_a=\sum_{s=1}^{2}\sum_{\alpha=1}^{N_s}\vec{P}_s^\alpha\psi_a(\vec{R}_s^\alpha). \tag{A1}$$

The coarse-grained free-energy functional F is defined as

$$e^{-\beta F}=\int \delta x\,\delta p\,e^{-\beta H}\prod_{a,s}\delta^{\mathrm{k}}\left(\rho_{sa}-\sum_{\alpha=1}^{N_s} m_s\psi_a(\vec{R}_s^\alpha)\right)\times\prod_a \delta\left[\vec{g}_a-\sum_{s=1}^{2}\sum_{\alpha=1}^{N_s}\vec{P}_s^\alpha\psi_a(\vec{R}_s^\alpha)\right], \tag{A2}$$

where we have used the notation

$$\int \delta x\,\delta p=\prod_{s=1}^{2}\sum_{N_s=0}^{\infty}\frac{1}{N_s!}\prod_{\alpha=1}^{N_s} d\vec{R}_s^\alpha d\vec{P}_s^\alpha . \tag{A3}$$

H is the Hamiltonian for the binary system

$$H=\sum_{s=1}^{2}\sum_{\alpha=1}^{N_s}\frac{P_s^{\alpha 2}}{2m_s}+U(\vec{R}_s^\alpha), \tag{A4}$$

where U is the interaction term and is a function of the spatial coordinates R_s^α denoting the position of the ath particle of the sth species in the mixture.

Using integral representation for Kronekal delta, δ^{k},

$$\delta^{\mathrm{k}}\left(\rho_{sa}-\sum_{\alpha=1}^{N_s} m_s\psi_a(\vec{R}_s^\alpha)\right) = \oint\frac{dz_{sa}}{2\pi\iota z_{sa}}\exp\left[\iota\left(\rho_{sa}-\sum_{\alpha=1}^{N_s} m_s\psi_a(\vec{R}_s^\alpha)\right)\ln z_{sa}\right] \tag{A5}$$

and for Dirac delta δ,

$$\delta\left[\vec{g}_a-\sum_{s=1}^{2}\sum_{\alpha=1}^{N_s}\vec{P}_s^\alpha\psi_a(\vec{R}_s^\alpha)\right] = \int_{-\infty}^{\infty}\frac{d\zeta_a}{(2\pi)^3}\exp\left(\iota\zeta_a\cdot\vec{g}_a-\sum_{s=1}^{2}\sum_{\alpha=1}^{N_s}\zeta_a\cdot\vec{P}_s^\alpha\psi_a(\vec{R}_s^\alpha)\right) \tag{A6}$$

in Eq. (A2), we obtain

$$e^{-\beta F}=\prod_{s=1}^{2}\prod_a\oint\frac{dz_{sa}}{2\pi\iota z_{sa}}\int_{-\infty}^{\infty}\frac{d\vec{\zeta}_a}{(2\pi)^3}\times\exp[\iota(\vec{\zeta}_a\cdot\vec{g}_a+\rho_{sa}\ln z_{sa})+\phi(z,\zeta)]. \tag{A7}$$

The function ϕ (z,ζ) is obtained as

$$e^{\phi(z,\zeta)}=\int \delta x\,\delta p\,e^{-\beta H}\exp\left[-\iota\sum_{s=1}^{2}\sum_{\alpha=1}^{N_s}(m_s\ln z_s(\vec{R}_s^\alpha) +\vec{P}_s^\alpha\cdot\vec{\zeta}(\vec{R}_s^\alpha))\right], \tag{A8}$$

and here we have substituted

$$\ln z_s(\vec{R}_s^\alpha)=\sum_a \ln z_{sa}\psi_a(\vec{R}_s^\alpha),$$

$$\vec{\zeta}(\vec{R}_s^\alpha)=\sum_a \vec{\zeta}_a\psi_a(\vec{R}_s^\alpha). \tag{A9}$$

After performing the momentum integral in Eq. (A8), we get

$$e^{\phi(\xi_s)}=\prod_{s=1}^{2}\left[\frac{2\pi m_s}{\beta}\right]^{3N_s/2}\int \delta x\,e^{-\beta U(R_s^\alpha)}\times\prod_{\alpha=1}^{N_s}\exp(-\iota m_s\ln\xi_s(\vec{R}_s^\alpha), \tag{A10}$$

with

$$\xi_s(\vec{R}_s^\alpha)=z_s(\vec{R}_s^\alpha)\exp\left[-\frac{\iota}{2\beta}\zeta_a^2\right]. \tag{A11}$$

Using Eqs. (A9), (A10), and (A11) in Eq. (A7), we obtain

$$e^{-\beta F}=\prod_{s=1}^{2}\prod_a\oint\frac{d\xi_{sa}}{2\pi\iota\xi_{sa}}\int_{-\infty}^{\infty}\frac{d^3\zeta_a}{(2\pi)^3}\times\exp\left[\iota\left(\vec{\zeta}_a\cdot\vec{g}_a-\frac{\rho_a}{2\beta}\zeta_a^2\right)+\theta(\xi_s)\right], \tag{A12}$$

where

$$e^{\theta(\xi_s)}=\prod_{s=1}^{2}\left(\frac{2\pi m_s}{\beta}\right)^{3N_s/2}\int \delta x\,\exp\Bigg[-\beta U(R_s^{\alpha})-\iota\sum_{\alpha=1}^{N_s}\left\{m_s\ln\xi_s(\vec{R}_s^{\alpha})-\sum_a \rho_{sa}\ln\xi_{sa}\right\}\Bigg]. \tag{A13}$$

The total density inside the ath cell is written as $\rho_a=\rho_{1a}+\rho_{2a}$. Calculating integrals on the ζ variable in Eq. (A12), we obtain

$$e^{-\beta F}=\prod_{s\,a}\left(\frac{\beta}{2\pi\rho_a}\right)^{3/2}\oint\frac{d\xi_{sa}}{2\pi\iota\xi_{sa}}\times\exp\left(-\frac{\beta}{2}\sum_a\frac{g_a^2}{\rho_a}+\theta(\xi_s)\right). \tag{A14}$$

In the coarse-grained free energy F the term $\Sigma_a g_a^2/2\rho_a$ reduces in the continuum limit, i.e., $\delta\rightarrow 0$ and $a\rightarrow\infty$, to the form (2.5) in Sec. III. For the interaction term, after integrating over the momentum $\vec{g}$ and substituting for $e^{\theta(\xi_s)}$ from Eq. (A13), the integral in Eq. (A12) can be written as

$$e^{\beta F_u}=\prod_{s=1}^{2}\left(\frac{2\pi m_s}{\beta}\right)^{3N_s/2}\int \delta x\,e^{-\beta U(R_s^{\alpha})}\times\prod_a \delta^{\mathrm{k}}\left(\rho_{sa}-\sum_{a=1}^{N_s}m_s\psi_a(\vec{R}_s^{\alpha})\right)=\prod_s\left[\frac{2\pi m_s}{\beta}\right]^{3N_s/2}e^{\beta\overline{F}_u}. \tag{A15}$$

The integral over the spatial variables is approximated in terms of occupation numbers of the cells, $n_{sa}=\rho_{sa}/m_s$ as

$$\exp(-\beta\overline{F}_u)=\prod_{a\,s}\frac{\delta^{n_{sa}}}{n_{sa}!}e^{-\beta\overline{U}(n_{sa})}, \tag{A16}$$

where $\overline{U}$ represents the effect of interaction term in the Hamiltonian. We have considered for $\overline{U}$ in Sec. II a standard Gaussian form in terms of direct correlation functions. One reaches the result

$$-\beta F_u=-\beta\overline{U}+\sum_s\sum_a\left[n_{sa}\ln\delta-n_{sa}\ln n_{sa}+n_{sa}-\frac{3n_{sa}}{2}\ln\left(\frac{2\pi m_s}{\beta}\right)\right], \tag{A17}$$

which in the continuum limit reduces to the form

$$\beta F_u=\sum_{s=1}^{2}\frac{1}{m_s}\int d^3x\,\rho_s(x)\left[\ln\frac{\rho_s(x)}{\rho_{0s}}-1\right]+\beta\overline{U}. \tag{A18}$$

The first term on the right side is present in absence of any interaction and represents the ideal-gas contribution to the free-energy.

[1] B. Kim and G.F. Mazenko, Adv. Chem. Phys. **78**, 129 (1990).
[2] M. Mezard, G. Parisi, and M.A. Virasoro, *Spin Glasses Theory and Beyond*, World Scientific Lecture Notes in Physics Vol. 9 (World Scientific, Singapore 1987).
[3] M. Mezard and G. Parisi, J. Phys.: Condens. Matter **12**, 6655 (2000).
[4] Walter Kob and H.C. Andersen, Phys. Rev. E **51**, 4626 (1995); **52**, 4134 (1995); Phys. Rev. Lett. **73**, 1376 (1994); J. Matsui, T. Odagaki, and Y. Hiwatari, *ibid.* **73**, 2452 (1994).
[5] J.J. Ullo and S. Yip, Phys. Rev. Lett. **54**, 1509 (1985); C.A. Angell, J.H.R. Clark, and L.V. Woodcock, Adv. Chem. Phys. **48**, 398 (1981); L.V. Woodcock and C.A. Angell, Phys. Rev. Lett. **47**, 1129 (1981).
[6] U. Krieger and J. Bosse, Phys. Rev. Lett. **59**, 1601 (1987); J. Bosse and J.S. Thakur, *ibid.* **59**(9), 998 (1987).
[7] J.L. Barrat and A. Latz, J. Phys.: Condens. Matter **2**, 4289 (1990).
[8] Markus Nauroth and Walter Kob, Phys. Rev. E **55**, 657 (1996).
[9] T.R. Kirkpatrick and J.C. Nieuwoudt, Phys. Rev. A **33**, 2658 (1986).
[10] S.P. Das and Gene F. Mazenko, Phys. Rev. A **34**, 2265 (1986).
[11] J.S. Langer and L.A. Turski, Phys. Rev. A **8**, 3230 (1973).
[12] T.V. Ramakrishnan and M. Yussouff, Phys. Rev. B **19**, 2775 (1979).
[13] Claude Cohen, J.W.H. Sutherland, and J.M. Deutch, Phys. Chem. Liq. **2**, 213 (1971).
[14] N. H. March and M. P. Tosi, *Theory of Atomic Liquids* (Academic, London, 1976).
[15] M. Fuchs and A. Latz, Physica A **201**, 1 (1993).
[16] J.S. Thakur and J. Bosse, Phys. Rev. A **43**, 4378 (1991); **43**, 4388 (1991); J. Bosse, Z. Phys. B: Condens. Matter **103**, 357 (1997).
[17] U. Bengtzelius, W. Gő̋tze, and A. Sjő̋lander, J. Phys. C **17**, 5915 (1984).
[18] S.K. Ma and Gene F. Mazenko, Phys. Rev. B **11**, 4077 (1975).
[19] I.E. Dzyloshinskii and G.E. Volovick, Ann. Phys. (N.Y.) **125**, 67 (1980).
[20] Supurna Sinha and M.C. Marchetti, Phys. Rev. A **46**, 4942 (1992).
[21] J.P. Hansen and J.R. McDonald, *Theory of Simple Liquids* (Academic, London, 1976).
[22] The authors of Ref. [13] discuss the fluctuating hydrodynamic equation for the binary fluid at linear level. Here the variables chosen are pressure fluctuations $\delta p(\vec{r},t)$ and concentration

$c(\vec{r},t)$ instead of ρ and c. The dynamical equations used here are the same as those in the present theory once a change of variable is made and the chemical potential is identified as $\mu_s/m_s = \delta F_u/\delta \rho_s$. Here the dynamics with the set of slow variables including the energy fluctuations was considered and in this formulation also the noises in the different fluctuating equations are related. This is expressed in Eq. (5.20) of Ref. [13]. This is simply required to ensure that the equation for the density variable, namely, the continuity equation does not have any noise. In the present context we have a similar relation between the noises in the equations for ρ_1 and ρ_2.

[23] Gene F. Mazenko, Sriram Ramaswamy, and John Toner, Phys. Rev. A **28**, 1618 (1983).
[24] N.W. Ashcroft and David C. Langreth, Phys. Rev. **156**, 685 (1967).
[25] J.L. Lebowitz, Phys. Rev. **133**, A895 (1964).
[26] Shankar P. Das, J. Phys.: Condens. Matter **12**, 1 (2000).
[27] Rajeev Ahluwalia and Shankar P. Das, Phys. Rev. E **57**, 5771 (1998).
[28] J.L. Barrat, M. Baus, and J.P. Hansen, J. Phys. C **20**, 1413 (1987).
[29] Upendra Harbola and Shankar P. Das (unpublished).